THE JOURNAL OF BIOLOGICAL CHEMISTRY
Vol. 275, No. 47, Issue of November 24, pp. 36645–36652, 2000

Printed in U.S.A.

The Binding of a Glycoprotein 120 V3 Loop Peptide to HIV-1 Neutralizing Antibodies

STRUCTURAL IMPLICATIONS*

Received for publication, June 20, 2000, and in revised form, August 29, 2000
Published, JBC Papers in Press, August 29, 2000, DOI 10.1074/jbc.M005369200

Gang Wu‡§, Roger MacKenzie¶, Paul J. Durda‖, and Pearl Tsang‡**

From the ‡Department of Chemistry, University of Cincinnati, Cincinnati, Ohio 45221-0172, the ¶Institute for Biological Sciences, National Research Council, 100 Sussex Drive, Ottawa, Ontario K1A 0R6, Canada, and the ‖Department of Pathology, Massachusetts General Hospital, Boston, Massachusetts 02115

The structural and antigenic properties of a peptide ("CRK") derived from the V3 loop of HIV-1 gp120 protein were studied using NMR and SPR techniques. The sequence of CRK corresponds to the central portion of the V3 loop containing the highly conserved "GPGR" residue sequence. Although the biological significance of this conserved sequence is unknown, the adoption of conserved secondary structure (type II β-turn) in this region has been proposed. The tendency of CRK (while free or conjugated to protein), to adopt such structure and the influence of such structure upon CRK antigenicity were investigated by NMR and SPR, respectively. Regardless of conjugation, CRK is conformationally averaged in solution but a weak tendency of the CRK "GPGR" residues to adopt a β-turn conformation was observed *after* conjugation. The influence of GPGR structure upon CRK antigenicity was investigated by measuring the affinities of two cognate antibodies: "5023A" and "5025A," for CRK, protein-conjugated CRK and gp120 protein. Each antibody bound to all the antigens with nearly the same affinity. From these data, it appears that: (*a*) antibody binding most likely involves an induced fit of the peptide and (b) the gp120 V3 loop is probably conformationally heterogeneous. Since 5023A and 5025A are HIV-1 neutralizing antibodies, neutralization in these cases appears to be independent of adopted GPGR β-turn structure.

The principal neutralizing determinant (PND)[1] of HIV-1 has been mapped to the third hypervariable (V3) loop of the HIV-1 envelope protein, gp120 (1). PND-derived peptides are used as immunogens to elicit antibodies that possess HIV-1 virus neutralization capabilities (2, 3). The binding of neutralizing antibodies blocks virus entry into the host cell but does not prevent binding of HIV-1 to its primary cell receptor protein, CD4 (4, 5). Although the V3 loop represents an important target for the development of vaccines against AIDS, its high sequence variability also makes it a very problematic one (6). Nonetheless, the occurrence of the highly conserved residue sequence, "GPGR," at the tip of the V3 loop has raised the possibility that these residues make up a conserved secondary structural element in gp120. The function of such a structural element, if one exists, is presently unknown, however. The precise predicted secondary structure adopted by the GPGR residues is a type II β-turn (6, 7).

In order to determine whether the conserved GPGR sequence confers certain secondary structural tendencies upon this region of the V3 loop, numerous NMR studies were conducted upon a variety of V3 loop-derived peptides (8–21). These peptides were shown to have only low density populations of folded structure and to be conformationally averaged in solution. Despite the report of a "core" gp120 protein complex crystal structure, this complex was prepared using a form of gp120 which lacked most of the hypervariable loops including V3 (22). Information regarding the actual three-dimensional structure of the V3 loop in native gp120 is therefore still unavailable.

Due to the linear and flexible nature of V3 loop peptides in solution, a variety of methods have been employed to induce greater and presumably more "native" structure in previously studied V3 loop peptides. These methods included aminoisobutyric acid substitution (10), insertion into a viral coat protein (23), glycosylation (12–14), attachment to resin beads (24), cyclization of the peptide (15), and trifluoroethanol addition (14–19).

One particular method used previously to induce structure in short, linear peptides involves covalent attachment (or "conjugation") of the peptide to BPTI protein. Using this method, a nine-residue peptide derived from hemagglutinin (25) was shown to significantly affect the solution structure of this peptide after its conjugation to BPTI (26). Due to the well characterized NMR properties of BPTI protein (27–32) and the fact that no modification of the peptide or solvent conditions are required, we chose to employ this method in an attempt to induce greater CRK peptide structure for these solution NMR studies.

We began NMR and surface plasmon resonance (SPR) studies of a PND peptide in order to investigate the structural propensities of this peptide (while free and conjugated to BPTI), and their potential importance to the binding of this peptide by HIV-1 neutralizing antibodies. The PND peptide of

* This work was supported by National Institutes of Health, NIGMS Grant GM-47013. The costs of publication of this article were defrayed in part by the payment of page charges. This article must therefore be hereby marked "*advertisement*" in accordance with 18 U.S.C. Section 1734 solely to indicate this fact.

§ Present address: University of Texas Medical School at Houston, Dept. of Internal Medicine, Div. of Hematology, 6431 Fannin, TX 77030.

** To whom correspondence should be addressed: Dept. of Chemistry, University of Cincinnati, P.O. Box 210172, Cincinnati, OH 45221-0172. Tel.: 513-556-2301; Fax: 513-556-9239; E-mail: pearl.tsang@uc.edu.

[1] The abbreviations used are: PND, principal neutralizing determinant; HIV-1, human immunodeficiency virus-1; SPR, surface plasmon resonance; FPLC, fast protein liquid chromatography; BPTI, bovine pancreatic trypsin inhibitor; DQ, double quantum spectroscopy; DQF-COSY, double quantum filtered correlated spectroscopy; DSS, 3-(trimethylsilyl)propanesulfonic acid; Fab, antibody antigen-binding fragment; FAB, fast atom bombardment; NOE, nuclear Overhauser effect; NOESY, nuclear Overhauser enhancement spectroscopy; OMIU, *o*-methylisourea; SPDP, *N*-succinimidyl-3-(2-pyridyldithio)propionate; TOCSY, total correlated spectroscopy; gp, glycoprotein; RU, resonance unit.

interest, "RK," has the following sequence: Arg^1-Ile^2-Gln^3-Arg^4-Gly^5-Pro^6-Gly^7-Arg^8-Ala^9-Phe^{10}-Val^{11}-Thr^{12}-Ile^{13}-Gly^{14}-Lys^{15}. This sequence, corresponding to residues 308–322 of the gp120 envelope protein of HIV-1 (using the gp120 numbering scheme for strain IIIB, Ref. 33), comprises the tip of the gp120 V3 loop and represents the center of the HIV-1 PND. The two antibodies studied, "5023A" and "5025A" were both raised against RK and both exhibit HIV-1 virus neutralization as well as cell fusion inhibition capabilities *in vitro* (33). Since a cysteinylated peptide was needed for the protein conjugation study, the free and BPTI-conjugated form of an N-terminal cysteinylated form of RK ("CRK") were actually studied and compared by NMR techniques.

To determine the overall importance of folded CRK structure to its binding by its cognate antibodies, 5023A and 5025A, SPR techniques were used to measure the binding of these antibodies to various forms of the CRK antigen- free CRK peptide, BPTI-conjugated CRK peptide, and intact gp120. Based upon the NMR and SPR data presented in this study, the relationship between peptide antigenic structure *versus* antibody binding preference (for this PND peptide and these antibodies) is then discussed.

EXPERIMENTAL PROCEDURES

Peptide Synthesis—A N-terminal cysteinylated form of peptide RK known as CRK, Cys^{-1}-Arg^1-Ile^2-Gln^3-Arg^4-Gly^5-Pro^6-Gly_7-Arg_8-Ala^9-Phe^{10}-Val^{11}-Thr^{12}-Ile^{13}-Gly^{14}-Lys^{15}, was synthesized and studied. The cysteine residue was required for conjugation of RK peptide to BPTI protein via a heterobifunctional chemical linker. This 16-residue peptide was synthesized using a Rainin Automated PS-3 Peptide Synthesizer and Fmoc chemistry. The crude peptide was purified using a Rainin HPXL HPLC System equipped with a Rainin Dynamax-300A reverse phase column with acetonitrile as the elution solvent. The peptide composition was verified by amino acid analysis and its molecular weight by FAB mass spectroscopy (Multiple Peptide Systems, San Diego, California). The peptide sequence and its purity (>95%) were evaluated by two-dimensional NMR techniques.

BPTI Modification and Peptide Coupling—The modification of BPTI and its coupling to CRK peptide was accomplished according to the method developed by Ebina *et al.* (34) with modifications. BPTI was modified using OMIU and then covalently linked to the chemical linker, SPDP, before peptide coupling. The modification of BPTI proceeds by conversion of its lysine residues to homoarginines. As a result, the N-terminal amino group remains as the only free amino group available for SPDP coupling. The cysteinyl side chain of the peptide is covalently attached to this linker. The protein was modified using *o*-methylisourea and then purified using a Amersham Pharmacia Biotech LKB FPLC system and a Mono-S ion exchange column. A NaCl salt gradient in a 20 mM glycine, pH 10.5, buffer was used to purify the modified protein. The main protein fraction, which eluted at NaCl concentrations greater than 0.54 M, was collected. This fraction was then dialyzed extensively against deionized, distilled water and subsequently lyophilized. The molecular weight of the OMIU-modified BPTI (OMIU-BPTI) was determined via matrix-assisted laser desorption/ionization-time of flight mass spectroscopy to be 6681 (*versus* 6513 for native BPTI), the expected mass for correctly modified BPTI. Amino acid analysis also conducted upon this protein further verified that conversion of the lysine side chains had been achieved. CRK peptide was then coupled via its terminal cysteine side chain to OMIU-BPTI using the cross-linker, SPDP. A disulfide bond between the peptide cysteine sulfhydryl group and linking reagent (shown in brackets below) is formed to produce the final protein-peptide conjugate: BPTI-NH-{CO-CH_2-CH_2-S}-S-Cys-RK Peptide. "BPTI-CRK" is the abbreviation used to denote CRK peptide conjugated to OMIU-BPTI. The conjugate was then purified using an FPLC and a Mono-S column. The conjugate was eluted using a 0–100% 1 M NaCl gradient in 100 mM sodium phosphate, pH 7.5. The conjugate eluted at ~0.95 M NaCl with this gradient and the fraction collected at this salt concentration was then dialyzed against 0.1 M NaCl followed by de-ionized, distilled water via ultrafiltration and an Amicon YM-3 membrane.

NMR Sample Preparation—NMR samples of CRK peptide, OMIU-BPTI, and BPTI-CRK peptide conjugate were prepared in 90% H_2O, 10% D_2O solutions at pH 4.1 with typical sample volumes of 0.5 ml. The various sample concentrations were 5.7 mM(CRK), 6.0 mM (modified BPTI), and 5.9 mM (BPTI-CRK). The pH of all NMR samples (uncorrected for deuterium isotope effects) was adjusted to 4.1 using DCl and NaOD solutions and an Orion520A pH meter. All proton resonances were ultimately referenced against DSS. To maintain the uncoupled cysteinylated peptide in its reduced state, dithiothreitol-d_6 was added to these samples using a molar ratio of dithiothreitol:peptide = 50:1.

NMR Spectroscopy—A Bruker DMX 500MHz spectrometer was used to acquire the NMR data presented. Standard NMR experiments and pulse sequences such as DQF-COSY (35, 36), NOESY (37), TOCSY (38), and double quantum experiments (39, 40) were used for assignment purposes. The water resonance was suppressed via the use of low level rf pulses applied at the beginning of the pulse sequence (usually 1.5 s long) and during the mixing time of a NOESY sequence. The sweep widths used were 5000–8012 Hz. The number of points collected was 8192 or 4096 during t_2 and 512 or 1024 points during t_1. For each t_1 point, 32 scans were acquired for all the NMR experiments. All NMR probe temperatures were calibrated using neat methanol (41).

The NMR data were processed using Felix 2.30 (Biosym Technologies, Inc.) software run either on a Silicon Graphics INDIGO R4000 or a Sun SPARCstation5 computer. Typical processed two-dimensional data matrices were 4 K by either 1 or 2 K. A $\pi/2$ phase-shifted sinebell window function was applied during F1 and F2 processing. Prior to F1 transformation, the first interferogram was multiplied by 0.5 to suppress t_1 ridges (42). The intensities of NOESY cross-peaks were measured by calculating the volumes of the cross-peaks as the integral of all the data point intensities within the cross-peak footprints. For the NOE intensity measurement of free and coupled peptides, the relative intensities of these NOEs were calibrated against the $d_{\alpha N}(i, i+1)$ NOE observed between the F10 Hα and V11 HN protons of each peptide.

Fab Preparation—Antibodies 5023A and 5025A were cleaved using papain and purified following standard procedures (43). All buffers were degassed before use and most steps in the procedure were conducted under N_2 gas. The enzyme and antibody solutions were mixed in a 1:100 papain:antibody ratio. The cleavage proceeded at 310 K for 12 h before the addition of iodoacetamide to a final concentration of 40 mM. This mixture was then incubated at 298 K for 1 h. The Fab was then dialyzed against a phosphate-buffered saline, pH 7.0, buffer using an Amicon and a YM30 membrane. The Fab fragment was purified with a FPLC system equipped with a Pharmacia 5-ml pre-packed protein A column using a pH 7.0 phosphate-buffered saline wash buffer and a 50 mM citrate, pH 3.0, elution buffer.

SPR Experiments—Binding kinetics were determined by SPR using a BIAcore 1000™ biosensor system (Biacore Inc., Piscataway, NJ) (44). The BPTI-peptide conjugate and gp120 (strain LAV, obtained from MicroGeneSys, Inc. via the NIH AIDS Research and Reference Reagent Program) were immobilized on research grade CM5 sensor chips at concentrations of 5 mg/ml in 10 mM sodium acetate, pH 4.5, for the conjugate and 10 mM sodium acetate, pH 6, for gp120 using the amine coupling kit supplied by the manufacturer. Approximately 150 resonance units of each conjugate and 2500 resonance units of gp120 were immobilized; one RU corresponds to an immobilized protein concentration of ~1 pg/mm^2 (45). Unreacted moieties on the surface were blocked with ethanolamine. The N-terminal cysteine of CRK was used to immobilize the peptide onto research grade CM5 sensor chips using a thiol-exchange coupling procedure. The carboxylated dextran surfaces of the sensor chips were first activated with *N*-hydroxysuccinimide and *N*-ethyl-*N*′-(dimethylaminopropyl)carbodiimide. Reactive disulfides were then introduced by reaction with 2-(2-pyridinyldithio)ethaneamine in 100 mM borate buffer, pH 8.5. The N-terminal cysteinylated peptide was then introduced at concentrations of 5 and 0.5 mg/ml, respectively, in 10 mM acetate buffer, pH 4.5. Finally, unreacted moieties on the surface were blocked with cysteine. All measurements of 5023A and 5025A Fab binding to the conjugate, gp120, and peptide surfaces were carried out in HEPES-buffered saline which contained 10 mM HEPES, pH 7.4, 150 mM NaCl, 3.4 mM EDTA. Analyses were performed at 298 K and flow rates of 30–50 ml/min. All surfaces were regenerated with 100 mM H_3PO_4.

SPR Data Analysis—Association and dissociation rate constants were calculated by numerical integration and global fitting to a 1:1 interaction model using BIAevaluation 3.0 software (Biacore, Inc.) and the equation: $dRU(t)/dt = k_aC(R_{max} - RU(t)) - k_dRU(t)$, where $RU(t)$ is the response at time t, R_{max} is the maximum response, C is the concentration of analyte in solution, k_a is the association rate constant, k_d is the dissociation rate constant, and $RU(0) = 0$.

TABLE I

Free and conjugated CRK ^1H chemical shift assignments

The proton resonances (in ppm) of free and conjugated CRK were assigned at pH 4.1 and 298 K. The free and conjugated CRK residues are represented using standard three-letter amino acid abbreviations, followed by N, where N corresponds to the residue number. Free and conjugated CRK residues are represented as "XxxN" and "CXxxN", respectively. The H_2O resonance (4.8 ppm at 298 K) is used as the internal frequency standard. Degenerate protons are indicated using a single chemical shift value. The chemical shift values of cis form resonances are italicized. Asterisk indicates that all the arginine $N^{\eta}H$ protons of free CRK were unresolvable. Overlap with BPTI resonances prevented assignment of the following conjugated CRK resonances: C-Arg^3 (cis form) side chain and all arginine $N^{\eta}H$ protons.

Residue	NH	αH	βH	Others
C-Cys^{-1}		4.39	3.27 & 3.18	
Cys^{-1}		4.29	3.12	
C-Arg^1	8.94	4.49	1.79	γH 1.62 δH 3.20 $N^{\varepsilon}H$ 7.23
Arg^1	8.81	4.47	1.82	γH 1.66 δH 3.22 $N^{\varepsilon}H$ 7.21 *$N^{\eta}H$ 6.69
C-Ile^2	8.38	4.17	1.81	γH 1.50 & 1.22 γCH_3 0.94 δCH_3 0.86
Ile^2	8.38	4.22	1.84	γH 1.51 & 1.22 γCH_3 0.90 δCH_3 0.87
C-Gln^3	8.57	4.40	2.05 & 1.96	γH 2.33 $N^{\varepsilon}H$ 7.52 & 6.88
Gln^3	8.57	4.42	2.09 & 1.99	γH 2.36 $N^{\varepsilon}H$ 7.54 & 6.88
C-Arg^4	8.51	4.41	1.82	γH 1.63 δH 3.18 $N^{\varepsilon}H$ 7.19
Arg^4	8.49	4.43	1.88 & 1.78	γH 1.67 δH 3.21 $N^{\varepsilon}H$ 7.21 *$N^{\eta}H$ 6.69
C-Gly^5	8.35	4.17 & 4.06		
	8.31	*4.05 & 3.84*		
Gly^5	8.34	4.30 & 4.05		
	8.31	*4.09 & 3.85*		
C-Pro^6		4.46	2.27	γH 2.03 δH 3.64
		4.63	*2.39 & 2.17*	γH *1.87* δH *3.60 & 3.53*
Pro^6		4.48	2.30 & 2.00	γH 2.06 & 2.01 δH 3.67
		4.64	*2.40*	γH *1.97* & *1.89 δH 3.57*
C-Gly^7	8.52	3.95		
	8.64	*4.00*		
Gly^7	8.52	3.97		
	8.64	*4.02*		
C-Arg^8	8.16	4.30	1.82 & 1.72	γH 1.59 δH 3.17 $N^{\varepsilon}H$ 7.19
	8.34	*4.31*		
Arg^8	8.16	4.33	1.82 & 1.74	γH 1.61 & 1.63 δH 3.20 & 3.21
	8.34	*4.33*	*1.85 & 1.72*	$N^{\varepsilon}H$ 7.18 *$N^{\eta}H$ 6.69
C-Ala^9	8.28	4.29	1.31	
Ala^9	8.27	4.31	1.32	
C-Phe^{10}	8.20	4.66	3.11 & 3.03	2,6H 7.22 3,5H 7.34 4H 7.28
Phe^{10}	8.19	4.67	3.15 & 3.03	2,6H 7.25 3,5H 7.37 4H 7.30
C-Val^{11}	8.08	4.19	2.03	γH 0.90
Val^{11}	8.08	4.21	2.05	γH 0.93
C-Thr^{12}	8.29	4.38	4.14	γH 1.20
Thr^{12}	8.28	4.35	4.16	γH 1.21
C-Ile^{13}	8.26	4.22	1.80	γH 1.50 & 1.22 γCH_3 0.87 δCH_3 0.86
Ile^{13}	8.25	4.23	1.90	γH 1.52 & 1.24 γCH_3 0.96 δCH_3 0.89
C-Gly^{14}	8.50	3.97		
Gly^{14}	8.49	3.98		
C-Lys^{15}	7.89	4.23	1.84	γH 1.39 δH 1.68
				εH 3.00 NH_3^+ 7.53
Lys^{15}	7.87	4.23	1.86	γH 1.41 δH 1.71 εH 3.02 NH_3^+ 7.54 ϵH 3.02 NH_3^+ 7.54

RESULTS

Proton Resonance Assignments—Proton chemical shift assignments for uncoupled and BPTI-coupled CRK peptide (Table I) were made on the basis of DQF-COSY, TOCSY, and NOESY data obtained from these samples according to standard assignment procedures (46). The spin systems were established from DQF-COSY and TOCSY data, while sequential resonance assignments were determined from NOESY data collected on these samples. All resonance assignments reported here for the various peptide and BPTI forms were obtained at 298 K and pH 4.1.

In the uncoupled and coupled CRK peptide spectra (Table I), a major, as well as minor, set of resonances was observed for residues Gly^5 to Arg^8. Based upon the $d_{\alpha\alpha}(i, i+1)$ NOEs observed between the Hα protons of the minor form of Gly^5 and Pro^6 that were measured from D_2O samples of free CRK and peptide (data not shown), the minor resonances were attributed to the *cis* form of these peptides arising from *cis-trans* isomerization about the Gly^5-Pro^6 peptide bond. The amount of *cis* conformer present in both peptide forms was estimated to be close to 10%.

BPTI Modification and Peptide Coupling—Nearly complete proton resonance assignments for native,[2] OMIU-modified, and peptide-conjugated BPTI were obtained in order to determine whether chemical modification and peptide coupling significantly affected BPTI. This was accomplished via comparison of the native BPTI *versus* OMIU-BPTI HN and Hα resonance frequencies. Very few resonance frequency changes were observed for most BPTI residues regardless of BPTI form and most of these were less than 0.02 ppm. The largest changes (observed after linkage of SPDP to OMIU-modified BPTI) consisted of large frequency shifts involving the following protein resonances: the HN and Hα of Ala^{58} and the Hα of R1. The OMIU-modified Ala^{58} backbone resonances underwent substantial frequency changes due to peptide coupling: the NH, Hα resonances shifted from 8.05 (4.05) to 7.81 (4.13 ppm) after coupling. A corresponding R_1 Hα frequency shift from 4.36 ppm (OMIU-BPTI) to 4.58 ppm (BPTI-CRK) was also seen. Comparison of the modified *versus* peptide-conjugated BPTI R_1 amide HN frequency was not possible since the R_1 amino group is

[2] Upon request, we will provide the ^1H NMR assignments for native, OMIU-modified, and peptide-conjugated BPTI. Peptide J-coupling, temperature coefficient, and ROESY data will also be given upon request.

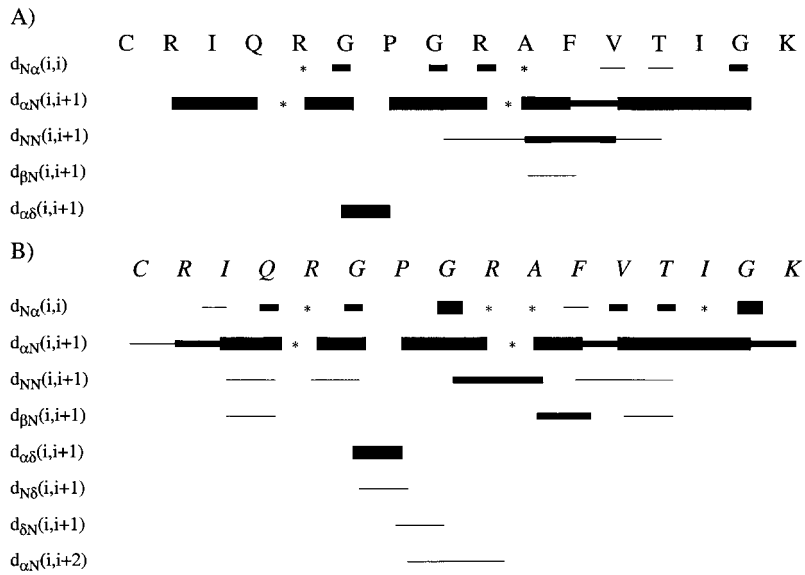

FIG. 1. **Backbone NOE connectivities observed for the free (*trans*) CRK (*A*) and coupled (*trans*) CRK (*B*).** These charts were based upon NOESY (500-ms mixing time) data recorded from these peptides at 500 MHz, 298 K, and pH 4.1. The *lines* drawn correspond to NOEs observed between the indicated protons and residues. Relative intensities of these NOEs are represented by relative *line thickness*. The $d_{\alpha\delta}(i, i+1)$ NOE between Gly^5 Hα and Pro^6 Hδ protons represent the average of the two $d_{\alpha N}(i, i)$ and $d_{\alpha\delta}(i, i+1)$ NOEs between the two nondegenerate Gly^5 Hα protons and the Pro^6 Hδ protons. The $d_{N\alpha}(i, i)$ of Gly^5 is the average of the two $d_{N\alpha}(i, i)$ NOEs between the two nondegenerate Gly^5 Hα protons and its HN proton. "*" indicates resonance overlap.

converted to an amide after peptide coupling.

Uncoupled Versus Coupled Peptide NOE Studies—The uncoupled peptide gave rise to medium-strong $d_{\alpha N}(i, i+1)$ NOEs involving residues Arg^1 through Gly^{14} (Fig. 1A). A weak $d_{\alpha N}(i, i+1)$ NOE was also observed between Arg^1 and Ile^2. At the same time, a few medium to weak $d_{NN}(i, i+1)$ NOEs were detected between residues Gly^7-Thr^{12}. Other sequential NOEs observed included a $d_{\beta N}(i, i+1)$ NOE between Ala^9 and Phe^{10}. In addition, strong $d_{\alpha\delta}(i, i+1)$ NOEs between both Gly^5 Hα protons and the Pro^6 Hδ proton were measured. Intraresidue $d_{N\alpha}(i, i)$ NOEs were observed for residues Gly^5, Gly^7, Val^{11}, Thr^{12}, and Gly^{14}. This type of NOE was also observed for Arg^8. The intraresidue $d_{N\alpha}(i, i)$ NOEs of Arg^4 and Ala^9 were overlapped with sequential $d_{\alpha N}(i, i+1)$ NOEs between Gln^3-Arg^4 and Arg^8-Ala^9, respectively.

As observed for the uncoupled peptide, most of the backbone protons of the coupled peptides gave rise to strong $d_{\alpha N}(i, i+1)$ NOEs (Fig. 1*B*). For coupled CRK peptide, $d_{NN}(i, i+1)$ NOEs were measured between sequential residues beginning with Ile^2-Thr^{12} (except Gln^3-Arg^4 and Ala^9-Phe^{10}). The strongest $d_{NN}(i, i+1)$ NOEs involved residues Gly^7-Ala^9. Furthermore, a weak Pro^6-Arg^8 $d_{\alpha N}(i, i+2)$ NOE was observed (Fig. 2*A*). For residue Pro^6, strong $d_{\alpha\delta}(i, i+1)$ NOEs between Gly^5 and Pro^6 were observed. Additionally, a $d_{N\delta}(i, i+1)$ NOE between the Gly^5 HN and Pro^6 Hδ protons was observed for coupled CRK. Another weak, but significant $d_{\delta N}(i, i+1)$ NOE between the Pro^6 Hδ and Gly^7 HN protons was also detected (Fig. 2*B*). Other sequential NOEs observed included $d_{\beta N}(i, i+1)$ NOEs between residues Ile^2-Gln^3, Ala^9-Phe^{10}, and Val^{11}-Thr^{12}. For the conjugated peptide, strong to medium intraresidue $d_{N\alpha}(i+1)$ NOEs were measured, except for residue Phe^{10}, for which a weak NOE of this type was measured instead. This type of NOE was not observed for Cys^{-1} and Arg^1. Intraresidue $d_{N\alpha}(i+1)$ NOEs of Arg^4 and Ala^9 were overlapped with $d_{\alpha N}(i, i+1)$ NOEs of Gln^3-Arg^4 and Arg^8-Ala^9, respectively. The corresponding Ile^{13} NOE was overlapped with an intramolecular BPTI NOE.

The β−turn NOEs observed for conjugated CRK were absent in the corresponding free peptide NOESY data, regardless of the mixing time (100–600 ms) used. To verify whether this discrepancy was a consequence of the peptide correlation time, free peptide ROESY data[2] were also collected (data not shown). The overall pattern of peptide resonances and the relative intensities of the free CRK cross-peaks measured were similar in the ROESY *versus* the NOESY data. Regardless of ROESY mixing time (50–300 ms, data not shown) used, GPGR β−turn cross-peaks were not observed at 298 K and 500 MHz in free CRK ROESY data. Since the NOESY and ROESY experiments were equally sensitive as far as detection of peptide cross-relaxation peaks, the NOESY experiment was employed since it allowed for better observation of BPTI resonances in the BPTI-CRK conjugate.

Antibody Binding Kinetics and Affinity Measurements—SPR was used to determine the kinetics and affinities of 5023A and 5025A binding to the following antigens: uncoupled and coupled CRK peptide and native gp120 protein. The SPR studies employed an antigen surface that was produced by immobilizing the antigen onto a dextran surface. The Fab (5023A or 5025A) was then flowed over this surface. Good fits to a 1:1 interaction model were obtained for most of the 5023A SPR sensorgram data. The overall quality of the fit is reflected in the relative errors of the affinity (K_{Aff}) constants derived from the sensorgram data. Table II summarizes the 5023A and 5025A K_{Aff} values, association (k_a) and dissociation (k_d) rates measured for all the antigens. By SPR, the affinities of both antibodies for RK and CRK were measured to be the same, within experimental error (data not shown). The 5023A and 5025A affinities for RK peptide (data not shown) were similar to those published earlier and determined by modified enzyme-linked immunosorbent assay (47). It was determined from microcalorimetry experiments that 5023A and 5025A do not bind appreciably to BPTI (data not shown). Fig. 3 provides an example of the 5023A and 5025A sensorgram data used to obtain the values listed in Table II.

The data for 5023A Fab binding to CRK and gp120 fit well to a 1:1 interaction model but the data for 5023A Fab binding to BPTI-CRK gave somewhat inferior fits and larger errors (Table II). In general, the affinities for the various antigens were relatively high ($>10^8$ M^{-1}) and not dramatically different. The relative error associated with the measured CRK and gp120 affinities were both relatively low (~5% or less) indicating that the 7-fold higher affinity for CRK relative to gp120 is significant. The 5023A/BPTI-CRK affinity had the highest (~10%) relative error among all the measured affinities for both antibodies (see Table II). In terms of binding kinetics, the association rates for CRK and BPTI-CRK were all similar whereas the corresponding dissociation rates for these complexes differed considerably. The BPTI-CRK dissociation rate was nearly twice that of CRK and this accounts for the corresponding decreased BPTI-CRK antibody affinity. Despite the difference in gp120 *versus* CRK association rates, their dissociation rates were

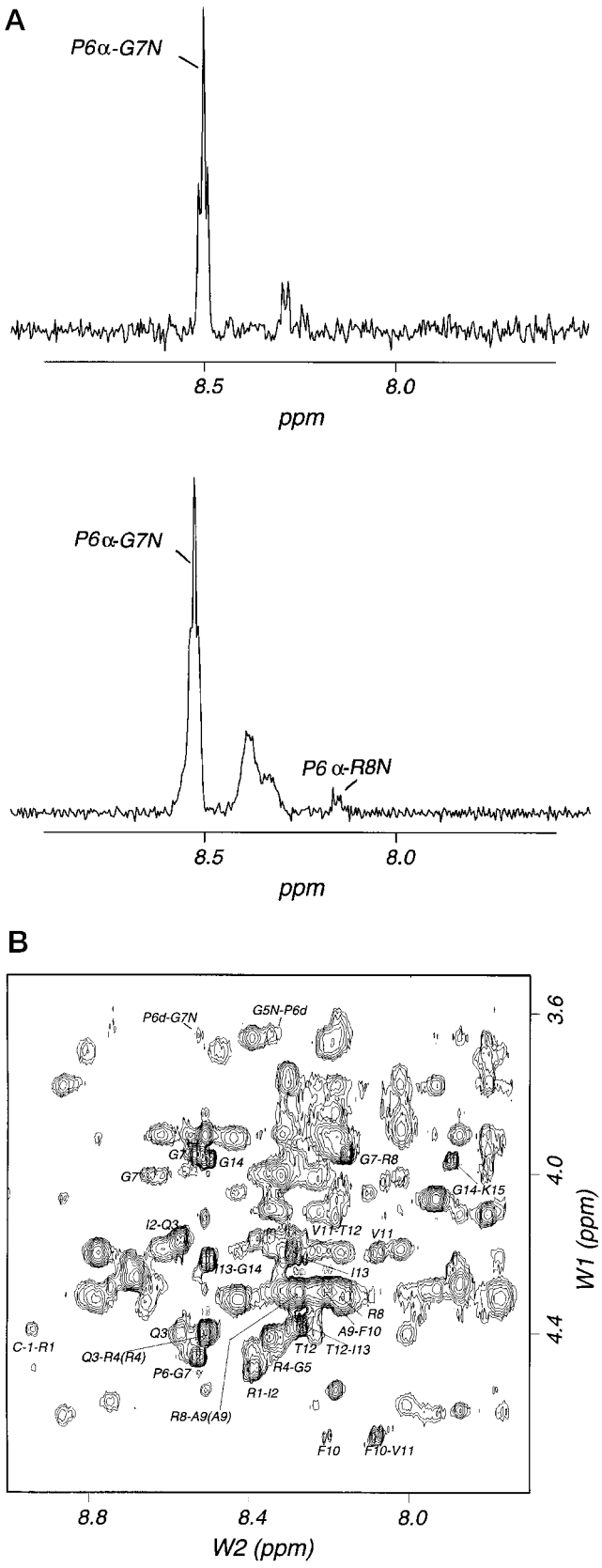

FIG. 2. **NOESY data recorded from free and coupled forms of CRK peptide at 500 MHz using a 500-ms mixing time.** *A*, *upper panel* corresponds to the f2 row at the Pro^6 Hα proton frequency in the NOESY spectrum of free CRK; *lower panel* is the analogous row in the NOESY data obtained from coupled CRK. The NOEs observed between the Pro^6 Hα and Gly^7 HN and the Pro^6 Hα to Arg^8 HN proton of the coupled peptide are indicated. *B,* fingerprint region of the NOESY spectrum. "$P_6\delta-G_7N$" corresponds to the $d_{\delta N}(i, i+1)$ NOE between Pro^6 Hδ and Gly^7 HN protons. "$G_5N-P_6\delta$" corresponds to the $d_{N\delta}(i, i+1)$ NOE between the Gly^5 HN and Pro^6 Hδ protons.

nearly the same. In either case, both of these antigens dissociated from the 5023A at a slower rate than did BPTI-CRK.

The Fab binding kinetics and affinity data obtained were more uniform in the case of 5025A with the binding to all three antigens fitting well to a 1:1 interaction model with low relative errors. The typical 5025A affinity (K_{Aff}) was approximately 10^6 M^{-1} and this was about 100-fold lower than the average 5023A affinity. The preferred order of 5025A binding, BPTI-CRK > CRK > gp120, should be accurate in view of the good fitting to the interaction model in each instance. Relative to gp120, the k_a and k_d rates for CRK peptide (regardless of conjugation state) binding were both somewhat faster.

DISCUSSION

BPTI Modification and Peptide Coupling—The largest effects observed upon BPTI due to peptide conjugation were restricted to the C- and N-terminal regions of BPTI. These effects were seen only after BPTI linkage to SPDP and consisted of substantial changes in the Ala^{58} and Arg^1 backbone resonance frequencies. At the pH (4.1) of these studies, a salt bridge exists between the α-amino group of Arg^1 and the C-terminal carboxylate group of residue Ala^{58} in native BPTI (48, 49). Since the α-amino (or N) terminus of BPTI becomes an amide group after BPTI reaction with SPDP, a relatively large (>0.2 ppm) shift of the BPTI Arg^1 Hα resonance occurred after SPDP coupling. Substantial shifts of the BPTI Ala^{58} Hα and HN resonances were also observed upon SPDP coupling and peptide linkage. The simultaneous occurrence of frequency changes involving the backbone Ala^{58} and Arg^1 resonances is consistent with disruption of the native BPTI Arg^1-Ala^{58} BPTI salt bridge due to conjugation of peptide to BPTI.

Since only minor NMR changes were observed for the remaining backbone resonances of BPTI after conjugation, the backbone of BPTI appears to be mostly unperturbed by such conjugation. This, along with the lack of significant CRK peptide resonance changes (regardless of peptide coupling), suggest that CRK and BPTI do not interact with each other significantly in the conjugate. This is supported by NOE build-up data for the free and conjugated forms of the peptide and BPTI (data not shown) which indicate that the overall correlation times (τ_c) of BPTI and CRK are not significantly affected by conjugation. The backbone CRK NOE maximum remains the same (regardless of conjugation to protein) and occurs at a much longer mixing time (400–500 ms, data not shown) compared with BPTI for which the NOE maximum remains between 100 and 150 ms (regardless of peptide coupling). However, relaxation studies of CRK peptide indicate that attachment of the peptide does affect CRK dynamics to some extent.[3]

Structural Tendencies of Uncoupled Versus BPTI-Coupled CRK Peptide—By NMR, free CRK peptide was determined to be mostly unstructured in solution. This is based upon the simultaneous observation of numerous, relatively strong sequential $d_{\alpha N}(i, i+1)$ NOEs and a few relatively weak $d_{NN}(i, i+1)$ NOEs throughout the peptide (50). In addition, the significant absence of medium- to long-range NOEs indicates that CRK adopts very little folded structure and that it undergoes extensive conformational averaging in solution. Other NMR evidence in support of such averaging was provided by the averaged $J_{N\alpha}$ constants[2] (5.7–7.7 Hz, data not shown) and

[3] Y. Sharma, L. Rosenblum, T. Elsass, and P. Tsang, manuscript in preparation.

TABLE II
5023A, 5025A Fab binding affinities (K_{Aff})

Antibody	Constant	Antigen		
		CRK	BPTI-CRK	gp120
5025A	k_a[a] (M^{-1} s^{-1})	2.4×10^4	2.2×10^4	2.9×10^3
	k_d (s^{-1})	4.1×10^{-3}	2.1×10^{-3}	1.1×10^{-3}
	K_{Aff} (M^{-1})/S.E.	5.9×10^6/0.5%	10.0×10^6/2.0%	2.6×10^6/1.8%
5023A	k_a (M^{-1} s^{-1})	7.6×10^5	2.5×10^5	9.9×10^4
	k_d (s^{-1})	6.0×10^{-4}	1.1×10^{-3}	5.0×10^{-4}
	K_{Aff} (M^{-1})/S.E.	13.0×10^8/5.2%	2.3×10^8/9.8%	2.0×10^8/4.5%

[a] k_d and k_a are the dissociation and association rates, respectively, and $K_{Aff} = k_a/k_d$.

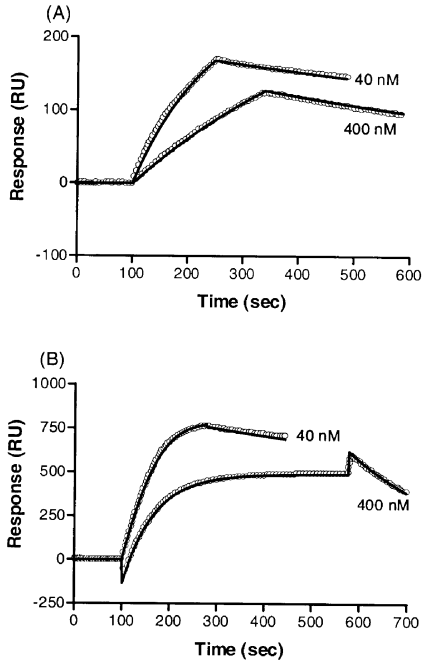

FIG. 3. **SPR sensorgrams showing the binding of 40 nM 5023A and 400 nM 5025A to immobilized gp120 (*A*) and CRK (*B*) and the fitting of the data to a 1:1 interaction model.** The data points are shown as *open circles* and the fitted lines in *solid black*.

relatively high values for the backbone amide proton temperature coefficients[2] (−5.3 to −9.1 ppb/K, data not shown). The strong intensities of the $d_{\alpha N}(i, i+1)$ NOEs are indicative of an extended peptide backbone. The peptide also exhibits a slight tendency to adopt some non-extended conformation involving residues Gly^7-Thr^{12}, based upon the weak $d_{NN}(i, i+1)$ NOEs observed for these residues.

The BPTI-coupled peptide NOEs also consisted primarily of strong backbone $d_{\alpha N}(i, i+1)$ NOEs and less frequently, weaker intensity $d_{NN}(i, i+1)$ NOEs. In cases where both NOE types were observed simultaneously, the relative intensity of the sequential $d_{\alpha N}(i, i+1)$ NOE was always much higher. The coupled peptide backbone was also mostly extended and the peptide was still conformationally averaged after BPTI coupling. Since $d_{NN}(i, i+1)$ NOEs were observed for residues Ile^2 to Thr^{12} in coupled CRK, the middle to N-terminal portion of the peptide backbone was less extended relative to the remainder of the peptide. An alternative explanation for the higher intensities of these particular $d_{NN}(i, i+1)$ NOEs may be that these residues are more motionally restricted due to their proximity to the protein attachment site.

In terms of NOEs specific to non-extended backbone structure, the coupled peptide Gly^7-Ala^9 $d_{NN}(i, i+1)$ NOEs were stronger relative to other $d_{NN}(i, i+1)$ NOEs and these residues therefore adopt non-extended conformations more readily. However, two new, but weak NOEs were observed for the coupled peptide. One of these corresponds to a $d_{\alpha N}(i, i+2)$ NOE between the Pro^6 Hα and Arg^8 HN protons, and it reflects a small β−turn tendency in the GPGR region. The second is a $d_{\delta N}(i, i+1)$ NOE between the Pro^6 Hδ and Gly^7 HN protons and it is further consistent with a type I β-turn in this region. However, the concurrent existence of a type II β-turn cannot be ruled out on the basis of these data alone since a strong $d_{\alpha N}(i, i+1)$ NOE between the Pro^6 Hα and Gly^7 HN protons was also observed. This latter NOE is characteristic of either a type II β-turn comprised of residues Gly^5 through Arg^8 or an extended backbone involving residues Pro^6 and Gly^7. Based on the relatively low intensity of this $d_{\alpha N}(i, i+2)$ NOE, the β-turn tendency is therefore significant but weak.

The $d_{\alpha N}(i, i+2)$ and $d_{\delta N}(i, i+1)$ cross-peaks were unobservable in NOESY and ROESY[2] data recorded from the free peptide. While it is possible that the GPGR turn tendency exists in the unconjugated peptide but was undetectable via NOESY due to peptide correlation time, these β-turn cross-peaks should still have been detected via the ROESY experiments that were also performed. Therefore, this structural tendency probably does not exist in the free peptide, or if it does, it is too weak for detection.

In contrast to an earlier study of a nonapeptide conjugated to BPTI (26), the conjugation of BPTI to CRK did not significantly affect the structural tendencies of CRK. This may simply reflect differences between these two peptides in terms of their inherent structural tendencies.

The NMR results reported here for uncoupled (or free) CRK peptide are consistent with other NMR investigations conducted by numerous groups upon a variety of V3 loop-derived peptides (8–21). The peptides studied varied somewhat in length (12–24 residues) and sequence but they all contained the highly conserved V3 loop GPGR residues. Typically, the overall tendency of these peptides to adopt a β-turn (of either type I or II) conformation in the GPGR region was relatively low. The peptides studied that were similar in length to CRK were shown to be primarily extended and mostly unfolded in solution. The relative intensities of the GPGR β-turn NOEs observed for other V3 loop peptides (similar to CRK in length) were comparable to those of coupled CRK peptide (see above). Therefore, the relative populations of β-turn structure adopted by those peptides *versus* coupled CRK in aqueous (without added trifluoroethanol) solution are about the same.

Antigen Structure versus Antibody Binding—The binding data indicate that 5025A antibody binds to both forms of CRK slightly better than gp120. For 5023A, the observed affinity differences are somewhat larger (<7-fold) and free CRK is preferred equally over the conjugated peptide and gp120 antigens. However, since the 5023A/BPTI-CRK sensorgram data fit least well to the interaction model, some caution must be exercised in interpretation of 5023A binding differences involving this antigen and others such as CRK, for example. The lower quality of the 5023A/BPTI-CRK SPR data is most likely attributable to effects upon 5023A binding due to heterogeneous

coupling of BPTI-CRK to the binding surface.

Since all the antigens (except CRK) were coupled via their amino groups, they were heterogeneously coupled to this surface. CRK was attached via its cysteine side chain, and was homogeneously coupled instead. Heterogeneous antigen coupling effects upon antibody binding are more significant for 5023A binding to the peptide conjugate than it is for gp120, since the latter has many more non-epitope amino groups available for surface immobilization.

Non-homogeneous antigen coupling to the surface can lead to complex binding behavior if coupling results in a mixture of fully and partially active antigen. This in turn will lead to complex Fab binding behavior and poorer fits of the obtained SPR data to simple interaction models. Such surface coupling heterogeneity is anticipated to yield SPR data with a faster than expected dissociation rate and a higher relative error for the value of the antibody affinity. Both of these phenomena were observed in the case of the 5023A/BPTI-CRK SPR data and the corresponding affinity. Therefore, the 5023A 7-fold binding difference between the different forms of CRK is probably not meaningful.

In contrast to 5023A, all the 5025A-conjugate sensorgram data were fit well to a 1:1 interaction model. Correspondingly, the relative errors obtained for the 5025A K_{Aff} values were all lower compared with those of 5023A. This discrepancy can be rationalized on the basis of differences in the 5023A and 5025A antigenic epitopes (47, 51). The 5023A RK epitope consists of residues Arg^4, Pro^6, Gly^7, Arg^8, Ala^9, Phe^{10}, Thr^{12}, and Gly^{14}, whereas the 5025A epitope is smaller and involves only residues Pro^6, Arg^8, Ala^9, and Phe^{10}. Since all the 5025A epitope residues are distant from both peptide coupling sites, heterogeneous coupling effects upon 5025A binding to the conjugate were probably much less significant. For 5023A, however, residue Gly^{14} is a 5023A epitope residue that is adjacent to Lys^{15}; hence 5023A binding to BPTI-CRK peptide could be hindered due to surface coupling of this peptide via its Lys^{15} side chain.

The differences in antibody binding to the various antigens (discussed above and summarized in Table II) were all meaningful, with the possible exception of the 5023A binding to CRK-BPTI data. However, all these binding differences were $<$10-fold and corresponded to $\leq$1 kilocalorie/mol affinity changes. Hence, antibodies 5023A and 5025A both exhibited no strong binding preference for any of the antigens, CRK, BPTI-CRK, and gp120.

To fully determine the structural basis for the antigenic binding differences observed for the 5023A/5025A antibodies, a detailed structural comparison between the intact gp120 V3 loop *versus* the 5023A/5025A antibody-bound state of the V3 loop (*i.e.* RK) peptide is really required. Such structural information regarding the V3 loop of gp120 (22), as well as the corresponding 5023A/5025A antibody-bound structures of gp120 and RK, are still unavailable, however. Nonetheless, general insight into this problem can still be derived from the structure and affinity data presented here. Based upon the fact that 5023A and 5025A are both cross-reactive (*i.e.* they bind to both the peptide and protein antigens), and that RK peptide is relatively unstructured in solution, there are at least three general schemes of anti-peptide antibody binding to consider as shown below (52). It is assumed in all cases that a substantial binding difference corresponds to a 10-fold or higher affinity change and that the antibody conformation remains the same, regardless of antigen binding. (*a*) If the anti-peptide antibody binds substantially better to native protein, the native protein structure is strongly preferred by this antibody. (*b*) If the anti-peptide antibody binds substantially better to the peptide than the native protein, unfolding of the protein is probably involved. The extent of such unfolding will be reflected by the extent to which the protein affinity is decreased relative to that of the peptide. (*c*) If the anti-peptide antibody binds the peptide and protein with nearly equal affinity, conformational differences between the protein and peptide are most likely small.

Typically, anti-peptide antibodies bind preferentially (and sometimes exclusively), to the "unfolded" protein fragment or peptide *versus* the folded protein (53–57). 5023A and 5025A are both anti-peptide antibodies raised against a protein-conjugated form of RK peptide. Both antibodies behaved "typically" in that they exhibited slightly higher affinities for the less structured peptide *versus* the native protein. This preference, however, was slight since the largest measured protein-peptide affinity difference corresponded to an energetic change of only about 1 kilocalorie/mol. Therefore, both antibodies exhibited essentially the same affinity for the protein and the peptide, regardless of conjugation. From the 5023A and 5025A affinity data, these antibodies are therefore examples of *c* above.

One of the simplest interpretations of the 5023A and 5025A binding data is that structural differences between CRK peptide and the corresponding V3 loop residue sequence in gp120 protein are probably small. Therefore, only small conformational changes of the protein may be required for its binding to 5023A and 5025A. CRK peptide was shown by NMR to adopt very little persistent structure. Hence the relevant residues in gp120 are also likely to be correspondingly unstructured and conformationally heterogeneous. This is entirely consistent with the fact that these residues are located in a loop region of gp120 protein.

Further evidence that the V3 loop is conformationally heterogeneous is provided by structural studies of various antibody-V3 loop peptide complexes (58–62). Structural comparison of two different V3 loop peptide-antibody complexes reveals that the structures adopted by the antibody-bound peptides in the two complexes were quite dissimilar and antibody-dependent (58, 60). This is despite the fact that both antibodies (0.5β and 59.1) neutralize the same strain of HIV-1 (IIIB) and therefore recognize and bind the same gp120 protein. Based upon these data, the $gp120_{IIIB}$ V3 loop (from which the CRK sequence is derived) is probably conformationally heterogeneous.

From further structural comparison of the antibody-bound *versus* unbound V3 loop peptides, it appears that the structure of the peptide was typically quite different in these two states (10, 58–62). This observation is also consistent with the observed lack of significant folded structure among the V3 loop peptides studied, as well as the important influence of the antibody upon the final antibody-bound structure adopted by these peptides.

For antibodies 5023A/5025A, CRK antigenicity does not appear to depend upon β-turn structure adopted in the GPGR region. This is based upon: 1) the relatively high affinity binding of these antibodies to CRK which is relatively unstructured, and 2) the fact that the small tendency of this peptide (in its conjugated state) did not significantly affect 5023A/5025A binding to the peptide. This is also consistent with the fact that the full epitopes recognized by these antibodies include most, but not all of the residues in the GPGR sequence (47, 51) and hence adoption of any particular structure in the GPGR region may be of less consequence to antibody binding. Also, since CRK lacks significant folded structure, the most likely scheme of peptide binding by antibodies 5023A and 5025A must involve an induced fit of this peptide to the binding sites of both antibodies.

In terms of HIV-1 virus neutralization, the binding of neutralizing antibodies to HIV-1 virus appears to somehow interfere with specific, but still unknown HIV-1 V3 loop binding

events that are required for infection (63). While the 5023A and 5025A antibodies are not necessarily representative of all HIV-1 neutralizing antibodies, it appears that their binding to HIV-1 is independent of the particular, folded structure adopted by the V3 loop GPGR residues. If a conserved structure adopted by these conserved residues is not crucial for 5023A/5025A neutralization of HIV-1, other possible functions for these residues should be considered. One proposed possibility is that this V3 region is directly involved in the binding and interaction between HIV-1 and co-receptor protein(s) (64). 5023A/5025A binding to this region may prohibit important co-receptor interactions involving these conserved gp120 residues. Another potential function of this conserved residue sequence may be that it serves as a recognition site for proteolysis of the V3 loop; specific cleavage of the V3 loop has been postulated to precede the cell membrane fusion events required for virus infection (61, 65–67). Flexibility of the V3 loop, especially involving the GPGR residues, would also be beneficial in this situation (66). For this latter possibility, 5023A/5025A binding to a particular region of the V3 loop could serve to prohibit access to this critical cleavage site (68).

Acknowledgments—The AIDS Research and Reference Reagent Program, Division of AIDS, NIAID, National Institutes of Health, provided the reagent LAV (IIIB), gp120 (from MicroGeneSys, Inc.). R. Dunlea, Y. Sharma, Dr. Hai-jun Sun, and T. Hirama are thanked for their suggestions and technical help. Drs. S. Lee, C. Caperelli, and H. Halsall are acknowledged for helpful discussions, and Dr. J. Osterhout for careful review of this manuscript.

Note Added in Proof—We acknowledge recent, relevant work by Huisman *et al.* (Huisman, J. G., Carotenuto, A., Labrijn, A. F., Papvoine, C. H. M., Laman, J. D., Schellekens, V. M., Koppelman, M. H. G. M., and Hilbers, C. W. (2000) *Biochemistry* **19,** 10866–10876) and Tugarinov *et al.* (Tugarinov, V., Zvi, A., Levy, R., Hayek, Y., Matsushita, S., and Anglister, J. (2000) *Structure* **8,** 385–395).

REFERENCES

1. Javaherian, J., Langlois, A. J., McDanal, C., Ross, K. L., Eckler, L. I., Jellis, C. L., Profy, A. T., Rusche, J. R., Bolognesi, D. P., Putney, S. D., and Matthews, T. J. (1989) *Proc. Natl. Acad. Sci. U. S. A.* **86,** 6768–6772
2. Palker, T. J., Clark, M. E., Langlois, A. J., Matthews, T. J., Weinhold, K. J., Randall, R. R., Bolognesi, D. P., and Haynes, B. F. (1988) *Proc. Natl. Acad. Sci. U. S. A.* **85,** 1932–1936
3. Goudsmit, J., Debouck, C., Meloen, R. H., Smit, L., Bakker, M., Asher, D. M., Wolff, A. V., Gibbs, C. J., Jr., and Gajdusek, D. C. (1988) *Proc. Natl. Acad. Sci. U. S. A.* **85,** 4478–4482
4. Wu, L., Gerard, N. P., Wyatt, R., Choe, H., Parolin, C., Ruffin, N., Borsetti, A., Cardoso, A. A., Desjardin, E., Newman, W., Gerard, C., and Sodroski, J. (1996) *Nature* **384,** 179–183
5. Trkola, A., Dragic, T., Arthos, J., Binley, J. M., Olson, W. C., Allaway, G. P., Cheng Mayer, C., Robinson, J., Maddon, P. J., and Moore, J. P. (1996) *Nature* **384,** 184–187
6. LaRosa, G. J., Davide, J. P., Weinhold, K., Waterbury, J. A., Profy, A. T., Lewis, J. A., Langlois, A. J., Dreesman, G. R., Boswell, R. N., Shadduck, P., Holley, H., Karplus, M., Bolognesi, D. P., Matthews, T. J., Emini, E. A., and Putney, S. D. (1990) *Science* **249,** 932–935
7. Hansen, J. E., Lund, O., Nielsen, J. O., Brunak, S., and Hansen, J. E. S. (1996) *Proteins Struct. Funct. Genet.* **25,** 1–11
8. Dettin, M., De Rossi, A., Autiero, M., Guardiola, J., Chieco-Bianchi, L., and Di Bello, C. (1993) *Biochem. Biophys. Res. Commun.* **191,** 364–370
9. De Lorimier, R., Moody, M. A., Haynes, B. F., and Spicer, L. D. (1994) *Biochemistry* **33,** 2055–2062
10. Ghiara, J. B., Ferguson, D. C., Satterthwaite, A. C., Dyson, H. J., and Wilson, I. A. (1997) *J. Mol. Biol.* **266,** 31–39
11. Gupta, G., Anantharamaiah, G. M., Scott, D. R., Eldridge, J. H., and Myers, G. (1993) *J. Biomol. Struct. Dyn.* **11,** 345–366
12. Huang, X., Smith, M. C., Berzofsky, J. A., and Barchi, J. J., Jr. (1996) *FEBS Lett.* **393,** 280–286
13. Huang, X., Barchi, J. J., Jr., Lung, F. T., Roller, P. P., Nara, P. L., Muschik, J., and Garrity, R. R. (1997) *Biochemistry* **36,** 10846–10856
14. Markert, R. L. M., Ruppach, H., Gehring, S., Dietrich, U., Mierke, D. F., Kock, M., Rubsamen-Waigmann, H., and Griesinger, C. (1996) *Eur. J. Biochem.* **237,** 188–204
15. Chandrasekhar, K., Profy, A. T., and Dyson, H. J. (1991) *Biochemistry* **30,** 9187–9194
16. Zvi, A., Hiller, R., and Anglister, J. (1992) *Biochemistry* **31,** 6972–6979
17. Vranken, W. F., Budesinsky, M., Martins, J. C. K., Boulez, K., Gras-Masse, H., and Borremans, F. A. M. (1996) *Eur. J. Biochem.* **236,** 100–108
18. Catasti, P., Fontenot, J. D., Bradbury, E. M., and Gupta, G. (1995) *J. Biol. Chem.* **270,** 2224–2232
19. Catasti, P., Bradbury, E. M., and Gupta, G. (1996) *J. Biol. Chem.* **271,** 8236–8242
20. Vu, H. M., de Lorimier, R., Moody, M. A., Haynes, G. F., and Spicer, L. D. (1996) *Biochemistry* **35,** 5158–5165
21. Vu, H. M., Myers, D., de Lorimier, R., Matthews, T. J., Moody, M. A., Heinly, C., Torres, J. V., Haynes, B. F., and Spicer, L. (1999) *J. Virol.* **73,** 746–750
22. Kwong, P. D., Wyatt, R., Robinson, J., Sweet, R. W., Sodroski, J., and Hendrickson, W. A. (1998) *Nature* **393,** 648–659
23. Jelinek, R., Terry, T. D., Gesell, J. J., Malik, P., Perham, R. N., and Opella, S. J. (1997) *J. Mol. Biol.* **266,** 649–655
24. Jelinek, R., Valente, A. P., Valentine, K. G., and Opella, S. J. (1997) *J. Mag. Reson.* **125,** 185–187
25. Dyson, H. J., Cross, K. J., Houghten, R. A., Wilson, I. A., Wright, P. E., and Lerner, R. A. (1985) *Nature* **318,** 480–483
26. Dyson, H. J. (1995) in *Immunological Recognition of Peptides in Medicine and Biology* (Zegers, N. D., Boersma, W. J. A., and Claassen, E., eds) pp. 133–145, CRC Press, Boca Raton, FL
27. Wagner, G., Braun, W., Havel, T. F., Schaumann, T., Go, N., and Wüthrich, K. (1987) *J. Mol. Biol.* **196,** 611–639
28. Beeser, S. A., Oas, T. G., and Goldenberg, D. P. (1998) *J. Mol. Biol.* **284,** 1581–1596
29. Balasubramanian, S., Nirmala, R., Beveridge, D. L., and Bolton, P. H. (1994) *J. Magn. Res. B* **104,** 240–249
30. Wagner, G., and Wüthrich, K. (1982) *J. Mol. Biol.* **155,** 347–366
31. Berndt, K. D., Guntert, P., Orbons, L. P. M., and Wüthrich, K. (1992) *J. Magn. Res.* **227,** 757–775
32. Nirmala, N. R., and Wagner, R. (1988) *J. Am. Chem. Soc.* **110,** 7557–7558
33. Durda, P. J., Bacheler, L., Clapham, P., Jenoski, A. M., Leece, B., Matthews, T. J., McKnight, A., Pomerantz, R., Rayner, M., and Weinhold, K. J. (1990) *AIDS Res.* **6,** 1115–1123
34. Ebina, S., Lerner, R. A., and Wright, P. E. (1989) *J. Mol. Biol.* **264,** 7882–7888
35. Rance, M., Sørensen, O. W., Bodenhausen, G., Ernst, R. R., and Wüthrich, K. (1983) *Biochem. Biophys. Res. Commun.* **117,** 479–485
36. Marion, D., and Wüthrich, K. (1983) *Biochem. Biophys. Res. Commun.* **113,** 967–974
37. Jeener, J., Meier, B. H., Bachmann, P., and Ernst, R. R. (1979) *J. Chem. Phys.* **71,** 4546–4553
38. Braunschweiler, L., and Ernst, R. R. (1983) *J. Magn. Reson.* **53,** 521–528
39. Rance, M., and Wright, P. E. (1986) *J. Magn. Reson.* **66,** 372–378
40. Rance, M., Chazin, W. J., Dalvit, C., and Wright, P. E. (1989) *Methods Enzymol.* **176,** 114–134
41. Van Geet, A. L. (1970) *Anal. Chem.* **42,** 679–680
42. Otting, G., Wider, H., Wagner, G., and Wüthrich, K. (1986) *J. Magn. Reson.* **66,** 187–193
43. Harlow, E., and Lane, D. (1988) in *Antibodies: A Laboratory Manual*, pp. 628–629, Cold Spring Harbor Laboratory, Cold Spring Harbor, NY
44. Jonsson, U., Fagerstam, L., Ivarsson, B., Johnsson, B., Karlsson, R., Lundh, K., Lofas, S., Persson, B., Roos, H., Ronnberg, I., Sjolander, S., Stenberg, E., Stahlberg, R., Urbaniczky, C., Ostlin, H., and Malmqvist, M. (1991) *Biotechniques* **11,** 620–627
45. Stenberg, E., Persson, B., Roos, H., and Urbaniczky, C. (1991) *J. Coll. Interface Sci.* **143,** 513–526
46. Wüthrich, K. (1986) *NMR of Proteins and Nucleic Acids*, John Wiley & Sons, New York, NY
47. Langedijk, L. P. M., Back, N. K. T., Durda, P. J., Goudsmit, J., and Meloen, R. H. (1991) *J. Gen. Virol.* **72,** 2519–2526
48. Brown, L. R., De Marco, A., Richarz, R., Wagner, G., and Wüthrich, K. (1978) *Eur. J. Biochem.* **88,** 87–95
49. Wlodawer, A., Nachman, J., Gilliland, G. L., Gallagher, W., and Woodward, C. (1987) *J. Mol. Biol.* **198,** 469–480
50. Dyson, H. J., and Wright, P. E. (1991) *Ann. Rev. Biophys. Biophys. Chem.* **20,** 519–538
51. Tsang, P., Mu, X., Wu, G., and Durda, P. J. (1997) *J. Mol. Recognit.* **10,** 256–261
52. Kim, P. S. (1988) *Biophys. Chem.* **31**, 107–111
53. Porter, R., and Whelan, J. (1986) *Ciba Found. Symp.* **119,** 70–74
54. Jemmerson, R. (1995) in *Immunological Recognition of Peptides in Medicine and Biology* (Zegers, N. D., Boersma, W. J. A., and Claassen, E., eds) pp. 213–225, CRC Press, Boca Raton, FL
55. Jemmerson, R. (1987) *Proc. Natl. Acad. Sci. U. S. A.* **84,** 9180–9185
56. Schwab, C., Twardek, A., Lo, T. P., Brayer, G. D., and Bosshard, H. R. (1993) *Protein Sci.* **2,** 175–182
57. Spangler, B. D. (1991) *J. Immunol.* **146,** 1591–1595
58. Ghiara, J. B., Stura, E. A., Stanfield, R. L., Profy, A. T., and Wilson, I. A. (1994) *Science* **264,** 82–85
59. Rini, J. M., Schulze-Gahmen, U., and Wilson, I. A. (1992) *Science* **255,** 959–965
60. Weliky, D. P., Bennett, A. E., Zvi, A., Anglister, J., Steinbach, P. J., and Tycko, R. (1999) *Nat. Struct. Biol.* **6,** 141–145
61. Tugarinov, V., Zvi, A., Levy, R., and Anglister, J. (1999) *Nat. Struct. Biol.* **6,** 331–335
62. Stanfield, R. L., Cabezas, E., Satterthwait, E. A., Profy, A. T., and Wilson, I. A. (1999) *Structure Fold Des.* **7,** 131–142
63. Ugolini, S., Mondor, I., Parren, P. W. H. I., Burton, D. R., Tilley, S. A., Klasse, P. J., and Sattentau, Q. J. (1997) *J. Exp. Med.* **186,** 1287–1298
64. Speck, R. F., Wehrly, K., Platt, E. J., Atchison, R. E., Charo, I. F., Kabat, D., Chesebro, B., and Goldsmith, M. A. (1997) *J. Virol.* **71,** 7136–7139
65. Clements, G. J., Price-Jones, M. J., Stephens, P. E., Sutton, C., Schulz, T. F., Clapham, P. R., McKeating, J. A., McClure, M. O., Thomson, S., Marsh, M., Kay, J., Weiss, R. A., and Moore, J. P. (1991) *AIDS Res.* **7,** 3–16
66. Johnson, M. E., Lin, Z., Padmanabhan, K., Tulinsky, A., and Kahn, M. (1994) *FEBS Lett.* **337,** 4–8
67. Hattori, T., Koito, A., Takatsuki, K., Kido, H., and Katunuma, N. (1989) *FEBS Lett.* **248,** 48–52
68. Niwa, Y., Mihiro, Y., Shiroh, F., Okumura, Y., and Hiroshi, K. (1996) *Eur. J. Biochem.* **237,** 64–70

The Binding of a Glycoprotein 120 V3 Loop Peptide to HIV-1 Neutralizing Antibodies: STRUCTURAL IMPLICATIONS

Gang Wu, Roger MacKenzie, Paul J. Durda and Pearl Tsang

J. Biol. Chem. 2000, 275:36645-36652.
doi: 10.1074/jbc.M005369200 originally published online August 30, 2000
